



Article

# Molecular Genetics of Pre-B Acute Lymphoblastic Leukemia Sister Cell Lines during Disease Progression

Hilmar Quentmeier \*, Claudia Pommerenke and Hans G. Drexler

Department of Human and Animal Cell Lines, Leibniz-Institute DSMZ—German Collection of Microorganisms and Cell Cultures, 38124 Braunschweig, Germany; claudia.pommerenke@dsmz.de (C.P.); Hans.Drexler101@t-online.de (H.G.D.)

\* Correspondence: hqu@dsmz.de; Tel.: +49-531-2616-165; Fax: +49-531-2616-150

**Abstract:** For many years, immortalized tumor cell lines have been used as reliable tools to understand the function of oncogenes and tumor suppressor genes. Today, we know that tumors can comprise subclones with common and with subclone-specific genetic alterations. We sequenced DNA and RNA of sequential sister cell lines obtained from patients with pre-B acute lymphoblastic leukemia at different phases of the disease. All five pairs of cell lines carry alterations that are typical for this disease: loss of tumor suppressors (*CDKN2A*, *CDKN2B*), expression of fusion genes (*ETV6-RUNX1*, *BCR-ABL1*, *MEF2D-BCL9*) or of genes targeted by point mutations (*KRAS* A146T, *NRAS* G12C, *PAX5* R38H). *MEF2D-BCL9* and *PAX5* R38H mutations in cell lines have hitherto been undescribed, suggesting that YCUB-4 (*MEF2D-BCL9*), PC-53 (*PAX5* R38H) and their sister cell lines will be useful models to elucidate the function of these genes. All aberrations mentioned above occur in both sister cell lines, demonstrating that the sisters derive from a common ancestor. However, we also found mutations that are specific for one sister cell line only, pointing to individual subclones of the primary tumor as originating cells. Our data show that sequential sister cell lines can be used to study the clonal development of tumors and to elucidate the function of common and clone-specific mutations.

**Keywords:** *MEF2D-BCL9*; *PAX5* R38H; pre-B-ALL



**Citation:** Quentmeier, H.; Pommerenke, C.; Drexler, H.G. Molecular Genetics of Pre-B Acute Lymphoblastic Leukemia Sister Cell Lines during Disease Progression. *Curr. Issues Mol. Biol.* **2021**, *43*, 2147–2156. <https://doi.org/10.3390/cimb43030149>

Academic Editor: Arumugam R. Jayakumar

Received: 4 November 2021

Accepted: 26 November 2021

Published: 30 November 2021

**Publisher's Note:** MDPI stays neutral with regard to jurisdictional claims in published maps and institutional affiliations.



**Copyright:** © 2021 by the authors. Licensee MDPI, Basel, Switzerland. This article is an open access article distributed under the terms and conditions of the Creative Commons Attribution (CC BY) license (<https://creativecommons.org/licenses/by/4.0/>).

## 1. Introduction

For many decades, cell lines have enabled the modeling of human disease in cell culture for a better understanding of a plethora of pathophysiological processes and also, most importantly, for drug screening. Clearly, cell lines represent a useful in vitro tool owing to their easy manipulability and reduced culture costs; furthermore, they constitute a renewable resource, and, provided they are grown under recommended conditions, they retain their characteristic features and the results are reproducible. Nevertheless, a detailed and fully annotated characterization is fundamental before their use. In fact, in many cancer research fields, cell lines offer the most comprehensively characterized platform [1,2].

Additionally, in the domain of hematopoietic tumors, cell lines represent vital and powerful models in experimental systems to unravel the pro-leukemogenic roles of specific genetic mutations. As all leukemia cell lines inevitably carry molecular alterations, it is also essential here for the utility of these models to appropriately detail these genomic changes [3].

Despite the achievement of a complete remission in the vast majority of patients with acute lymphoblastic leukemia (ALL), ALL relapse remains a leading cause of childhood cancer-related death [4]. Relapsed ALL is thought to always be clonally related to the disease at diagnosis. Prior studies suggest that clonal mutations at relapse emerge from relapse-favoring subclones that already existed at diagnosis [4]. Their actual molecular and cellular input to therapy resistance and relapse remain, however, incompletely understood.

The field of clonal evolution is an intensely discussed topic, both generally in cancer but also specifically in leukemia [5–7].

To obtain further insight into the relative impact of founding genomic alterations and acquired genetic alterations, we set out to examine the gene mutation status and gene expression of paired cell lines procured from ALL patients at diagnosis and at subsequent relapse or at other consecutive stages of their disease, aiming at a better understanding of the ALL relapse processes.

## 2. Material and Methods

### 2.1. Cell Lines

Cell lines NALM-20 and NALM-21 were taken from the stock of the cell lines bank (Leibniz Institut DSMZ—Deutsche Sammlung von Mikroorganismen und Zellkulturen GmbH, Braunschweig, Germany). All other cell lines were supplied for research purposes. Cell lines were authenticated by DNA profiling. Detailed references and cultivation protocols for NALM-20, NALM-27 and PC-53 have been described previously [8].

### 2.2. RNA-Sequencing Analysis

Total RNA was extracted via the miRNeasy Mini Kit (Qiagen, Hilden, Germany) including DNase digestion. Library preparation and sequencing steps were commissioned to GATC Biotech (Cologne, Germany). The GATC pipeline included the production of strand-specific (fr-first strand) mRNA libraries, quality control via Applied Biosystems Fragment Analyzer and Nanodrop, and concentration measurement via Qubit fluorometer. The libraries were sequenced on Illumina HiSeq2500 (2 × 151 cycles, paired end run, 8 bp dual indices) with >29 million reads per sample and deposited at ArrayExpress (E-MTAB-11038). Reads were trimmed via fastq-mcf (ea-utils 1.04.807), quality-controlled via FastQC ([www.bioinformatics.babraham.ac.uk/projects/fastqc](http://www.bioinformatics.babraham.ac.uk/projects/fastqc), accessed on 28 May 2019) and aligned by STAR (2.5.3a) [9] to the Gencode Homo sapiens genome (v26) and converted/sorted via samtools (0.1.19) [10]. Counting the reads to each gene was done via HTSeq-count python script (0.8.0) [11]. Data was processed and analyzed in the R/Bioconductor environment (3.3.2/3.3, [www.bioconductor.org](http://www.bioconductor.org)). Normalization, estimation of dispersions, and testing for differentially expressed genes based on a test assuming a negative binomial data distribution were computed via DESeq2 [12].

Fusion genes were detected by fusionCatcher (0.99.6a beta) ( $\geq 1$  min-split-read +  $\geq 3$  min-span-pairs; hg38) [13].

### 2.3. Whole Exome Sequencing (WES) Analysis

DNA was isolated with the High Pure PCR Template Preparation Kit (Roche Diagnostics, Mannheim, Germany). Library preparation (Agilent SureSelect Human All Exon V6, 60 MB) and sequencing steps (2 × 151 bp + 8 bp barcoding, HiSeqX) were commissioned to Genewiz (Leipzig, Germany) and deposited at ArrayExpress (E-MTAB-11039). Insert lengths were aimed to be higher than 250 bp in order to increase the coverage and uniformity in coding regions [14].

Reads were aligned by STAR (2.5.3a) [9] to the human gencode genome (v26). Subsequently, alignment files were processed (samtools 0.1.19), duplicates removed (picard 2.9.2, [www.broadinstitute.github.io/picard/](http://www.broadinstitute.github.io/picard/), accessed on 28 May 2019), and variants called via GATK tools (3.7, Haplotypecaller) [15] and overlapping VarScan (v2.4.3) [16] results. Mutation effects were annotated via Ensembl VEP (release-84, GRCh38) [17]. Data were processed and analyzed in the R/Bioconductor environment (3.3.2/3.3). Overlapping single nucleotide variations via Haplotypecaller and VarScan were filtered for  $\geq 20$  quality,  $\geq 10$  depth,  $\geq 0.2$  allele frequency,  $< 0.01$  MAF, and missense/frameshift/stop gained mutations.

#### 2.4. RT-PCR, Genomic PCR and Sanger Sequencing

cDNA was prepared using the SuperScript II reverse transcriptase kit (Invitrogen, Karlsruhe, Germany). PCR was performed for 36 cycles on a C1000 Thermal Cycler (Bio-Rad, Dreieich, Germany) with an annealing temperature of 59 °C. The PCR primers are listed in Supplementary Table S3 (See Supplementary Materials). After agarose gel electrophoresis, the PCR products were purified with the QIAquick gel extraction kit (Qiagen, Hilden, Germany) and Sanger-sequenced (Eurofins, Ebersberg, Germany).

#### 2.5. Numerical Aberrations

A CytoScan HD Array (Affymetrix, Santa Clara, CA, USA) hybridization analysis was performed to identify numerical aberrations. DNA was prepared using the Qiagen Genra Puregene Kit (Qiagen, Hilden, Germany). Data were analyzed using the Chromosome Analysis Suite software version 2.0.1.2 (Affymetrix).

### 3. Results

#### 3.1. Mutations and Chromosomal Aberrations

Encoding *ETV6-RUNX1*, t(12;21)(p13;q22) is the prevalent chromosomal rearrangement in pediatric B-ALL [18], detectable in 15–25% of cases [19]. We had found that 0/13 adult pre-B ALL cell lines and 1/13 pediatric pre-B ALL cell lines (REH) expressed the *ETV6-RUNX1* fusion, previously known as *TEL-AML1* [20].

The RNA-seq data analysis shows that AT-1 and sister cell line AT-2, obtained from a 5 year old boy with pre-B ALL at 1st and 2nd relapse [21], also express the *ETV6* exon 5/*RUNX1* exon 4 fusion (Table 1, Figure 1, Supplementary Figure S1A). The cell lines were also published as SUP-B26/SUP-B28. The reverse *RUNX1* exon 3/*ETV6* exon 6 fusion transcript is also present in both cell lines (Table 1, Figure 1, Supplementary Figure S1B). *ETV6-RUNX1* is commonly detectable at birth. Secondary events are obligatory to induce tumorigenesis [19]. *ETV6* is a partner of gene fusions but is also recurrently deleted in pre-B ALL [22]. Indeed, the *ETV6-RUNX1* positive cell lines AT-1 and AT-2 had lost one *ETV6* allele (Table 1). Thus, they express the fusion but not the wild-type form of *ETV6*.



**Figure 1.** Transcripts of fusion genes in pre-B ALL cell lines. *ETV6-RUNX1*, *RUNX1-ETV6*, *MEF2D-BCL9*, *BCL9-MEF2D* and *NSMAF-NUCKS1* RT-PCR products are shown, separated on an agarose gel.

**Table 1.** Mutations and genomic aberrations in pre-B ALL sister cell lines.

Copy Number	AT-1 (5y)	AT-2 (5y)	NALM-20 (62y)	NALM-21 (63y)	NALM-27 (38y)	NALM-30 (39y)	PC-53 (33y)	PC-53A (34y)	YCUB-4 (7y)	YCUB-4R (7y)
<i>BTG1</i> (12q21.33)	2n	2n	1n	1n	2n	2n	2n	2n	2n	2n
<i>BTLA</i> (3q13.2)	2n	2n	1n	1n	1n	1n	2n	2n	2n	2n
<i>CDKN2A</i> (9p21.3)	0n	0n	0n	0n	0n	0n	0n	0n	0n	0n
<i>CDKN2B</i> (9p21.3)	0n	0n	0n (partial)	0n (partial)	0n (partial)	0n (partial)	0n	0n	0n	0n
<i>ETV6</i> (12p13.2)	1n	1n	2n	2n	2n	2n	2n	2n	2n	2n
<i>IKZF1</i> (7p12.2)	2n	2n	0n (partial)	0n (partial)	0n (partial)	0n (partial)	2n	2n	2n	2n
<i>NR3C1</i> (5q31.3)	2n	2n	2n	2n	2n	2n	1n	1n	2n	2n
<i>PAX5</i> (9p13.2)	2n	2n	2n	2n	2n	1.5–2n	2n	2n	1n	1n
<i>TP53</i> (17p13.1)	2n	2n	2n	2n	2n	2n	1n	1n	2n	2n
<b>fusion transcripts</b>										
<i>BCR-ABL1</i>	no	no	yes	yes	yes	yes	no	no	no	no
<i>ETV6-RUNX1</i>	yes	yes	no	no	no	no	no	no	no	no
<i>MEF2D-BCL9</i>	no	no	no	no	no	no	no	no	yes	yes
<i>NSMAF-NUCKS1</i>	no	no	no	no	no	no	yes	no	no	no
<i>RUNX1-ETV6</i>	yes	yes	no	no	no	no	no	no	no	no
<b>point mutations</b>										
<i>KRAS</i> A146T	0/1 (85/15)	0/1 (50/50)	no	no	no	no	no	no	no	no
COSM19404										
<i>NRAS</i> G12C COSM561	0/1 (65/35)	0/1/ (97/3)	no	no	no	no	no	no	no	no
<i>PAX5</i> R38H										
COSM5986423	no	no	no	no	no	no	0/1	0/1	no	no

Aberrations and differences between sister cell lines are highlighted. Fusion transcripts were detected by analyzing RNAseq data with fusion\_catcher; all fusion transcripts are in frame. Numeric status by CGH analysis, point mutations by WES analysis. COSM numbers are legacy mutation identifiers identifying existing mutations: 0/1: wild type/mutant; 0/0: wild type/wild type; numbers in brackets (wild type reads/mutant reads).

t(9;22) fusing *BCR* and *ABL1* is the hallmark of chronic myelogenous leukemia (CML), but it also occurs in 3–5% of childhood B-ALL and in 25% of adult ALL cases [19]. NALM-20 and NALM-21 express the *BCR-ABL1* fusion transcript (Table 1) [23]. NALM-20 was raised from a 62-year-old patient at diagnosis and NALM-21 from the same patient at relapse. NALM-27 and NALM-30 are also *BCR-ABL1*-positive (Table 1) [24]. NALM-27 was raised from a 38 year old patient at diagnosis, and the sister cell line NALM-30 was derived at relapse [25].

In 2016, *MEF2D* translocations were described in pre B-ALL, with *BCL9* being the most common fusion partner of *MEF2D* [26]. YCUB-4 and the sister cell line YCUB-4R express the *MEF2D* exon 5/*BCL9* exon 9 fusion transcript, resulting from t(1;1)(q21.2;q22) (Table 1, Figures 1 and 2). These cell lines are from a 7 year old boy with pre-B ALL at diagnosis and relapse [27]. The *MEF2D-BCL9* fusion is not the only pre-B ALL characteristic genetic alteration in this pair of cell lines. YCUB-4 and YCUB-4R also show a hemizygous loss of *PAX5* (Table 1). *PAX5* deletions had been found in 56/192 B-progenitor ALL cases [28].

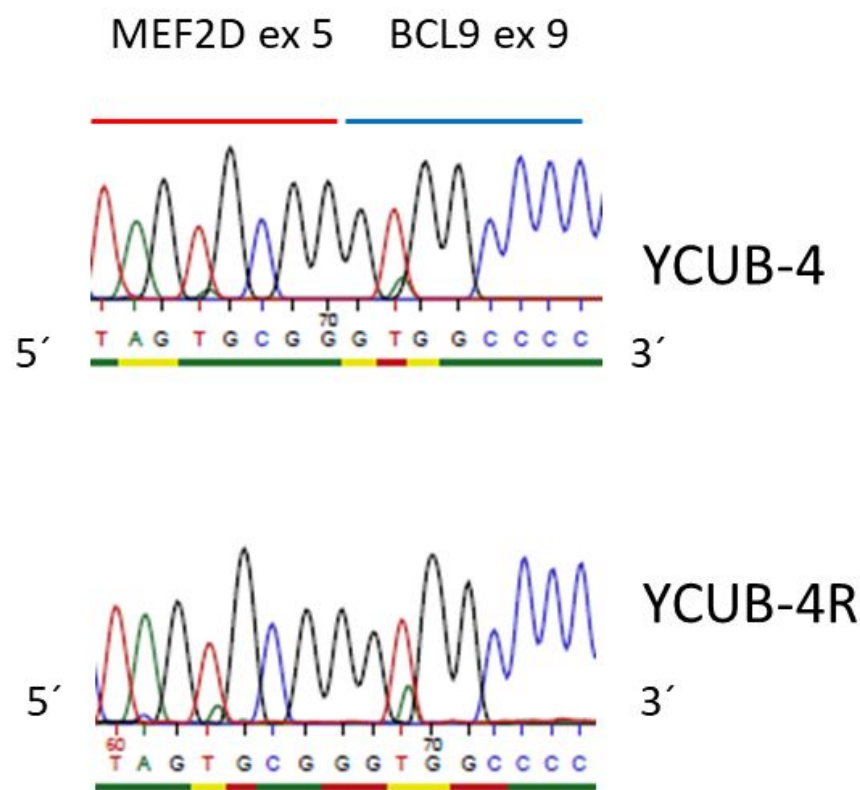


**Figure 2.** *MEF2D/BCL9* fusion mRNA. Pre-B ALL cell lines YCUB-4 and YCUB-4R express the *MEF2D* exon 5/*BCL9* exon 9 fusion transcript. The *MEF2D/BCL9* PCR product was sequenced with the *MEF2D* exon 5 forward primer (Supplementary Table S3). The fusion transcript is in frame.

*PAX5* is also a partner of translocations, and it is the target of point mutations in this disease [28,29]. PC-53, from a 33 year old woman with pre-B ALL at 3rd relapse and the sister cell line PC-53A (at the final, refractory stage) [30], carry the *PAX5* R38H mutation (Table 1, Figure 3). This mutation had been described in the context of pre-B ALL (COSM5986423). Additional mutations specifically occurring in one of the sister cell lines are shown in Supplementary Table S1 (exemplarily for chromosome 14). As assessed by a principal component analysis (PCA), the sister cell lines show closely related gene expression profiles (Supplementary Figure S2).

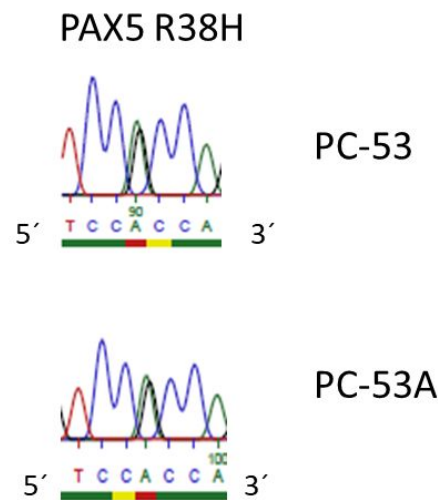


**Figure 3.** *PAX5* R38H mutation in PC-53 and PC-53A. Genomic PCR and sequencing show that the pre-B ALL cell lines PC-53 and PC-53 carry the *PAX5* R38H (cGc/cAc) mutation (0/1). Sequencing was performed with the *PAX5* intron 1/2 forward primer (Supplementary Table S3).

Focal deletions or sequence mutations of *IKZF1* are recurrent in pediatric ALL [19]. *IKZF1* can be lost as whole or can be subject to partial deletions [31]. NALM-20 and NALM-27, which were derived from two patients, show partial deletions of *IKZF1* (0n) along with their sister cell lines (Table 1, Supplementary Figure S3). Partial *IKZF1* deletions and deletions of *CDKN2A* and *CDKN2B* are markers of disease recurrence in adolescent and adult Philadelphia chromosome-negative pre-B ALL [32]. In pediatric ALL, two-thirds of *BCR-ABL1*-positive cases and a lower proportion (<5–25% depending on the subtype) of *BCL-ABL1*-negative cases carry the *IKZF1* deletion [33]. Noticeably, both pairs of cell lines with an *IKZF1* deletion are from adults and carry the *BCR-ABL1* fusion (Table 1). All five pairs of sister cell lines show deletions of *CDKN2A* and *CDKN2B* (Table 1, Supplementary Figure S4).

*BTG1*, *BTLA*, *NR3C1* and *TP53* are other genes that are recurrently deleted in pre-B ALL [19,32,34]. One allele of these genes is lost in at least one pair of our five sister cell line sets (Table 1).

None of the aberrations listed so far affected only one of the sister cell lines exclusively. Obviously, none of the mutations had developed during tumor progression. Therefore, the mutations described so far did not allow for a description of subclonal development. However, we found other mutations that indeed indicate that such a process did occur.

### 3.2. Subclonal Developments in Sister Cell Lines

The *NSMAF* (ex 1)—*NUCKS1* (ex 2) fusion is expressed in the cell line PC-53 but not in the sister cell line PC-53A (Table 1, Figure 1, Supplementary Figure S5). This fusion has not been reported in the context of pre-B ALL so far. However, the presence of *NSMAF-NUCKS1* in the earlier cell line and absence in the later suggests that *NSMAF-NUCKS1*-positive and -negative clones already existed when cell line PC-53 was raised. The results of the comparative genomic hybridization (CGH) analysis showed that in PC-53 both genes, *NSMAF* and *NUCKS1*, were located in the middle of the transition between two copy numbers (Supplementary Figure S6). These data localize the *NSMAF* and *NUCKS1* translocation breakpoints in cell line PC-53 at the appropriate chromosomal positions. PC-53A does not show these differences in copy numbers (Supplementary Figure S6). Thus, the sister cell lines exhibited molecular differences, providing an explanation for the exclusive expression of the *NSMAF-NUCKS1* (t(1;8)(q32.1;q12.1)) fusion transcript in PC-53 and not in PC-53A.

Because the CGH analysis was suitable for detecting molecular differences between the sister cell lines PC-53 and PC-53A, we performed copy number analyses to elucidate

whether other sister cell lines carried clone-specific copy number differences as well. Most aberrations detected by the CGH analysis were found in both of the sister cell lines (Supplementary Table S2; highlighted in green). In 4/5 sister pairs, we found aberrations in the later sister that were not present in the early sister (Supplementary Table S2; highlighted in red). However, we also detected aberrations in the earlier cell line that did not exist in the later cell line (Supplementary Table S2; highlighted in purple).

The WES data analysis indicated that the sister cell lines AT-1 and AT-2 consisted of subclones with *KRAS* A146T (Gca/Aca) or with *NRAS* G12C (Ggt/Tgt) mutations (Table 1). Both sister cell lines are diploid for these genes (Supplementary Figure S7). Therefore, one would expect 50% reads for the wild-type and mutant versions of the genes, respectively. In AT-2, 50% of reads of *KRAS* were wild type and 50% were mutant (*KRAS* A146T; Gca/Aca) (Table 1, Supplementary Figure S8). However, only 15% of the reads were mutant in cell line AT-1 (Table 1, Supplementary Figure S8). Furthermore, the reads for the *NRAS* mutation did not follow the expected 50% wild-type and 50% mutant scheme. In AT-1, 35% of reads encoding *NRAS* G12C (Ggt/Tgt) were mutant. In AT-2, 3% were mutant (Table 1, Supplementary Figure S9).

The easiest explanation for these results is that both sister cell lines comprise two subclones, “clone A” being *KRAS* homozygously wild-type (0/0)/*NRAS* heterozygously mutant (0/1) and “clone B” being *KRAS* (0/1)/*NRAS* (0/0). Table 2 shows the proportion of these subclones in the two sister cell lines based on read numbers and under the assumption that the subclones carry wild-type and mutant versions of the genes.

**Table 2.** The mutational analyses of *KRAS* and *NRAS* suggest that AT-1 and AT-2 are comprised of subclones.

Cell Line	Clone A <i>KRAS</i> (0/0)/ <i>NRAS</i> (0/1)	Clone B <i>KRAS</i> (0/1)/ <i>NRAS</i> (0/0)
AT-1	70%	30%
AT-2	<5%	>95%

Mutations were detected by WES analysis. (0/0) homozygously wild-type; (0/1) wild-type and mutant.

#### 4. Discussion

We have previously shown that B-lymphoma cell lines can comprise subclones [35]. Twelve percent of cell lines with immunoglobulin (IG) hypermutations (6/49) consisted of subclones with individual IG mutations [35]. The cell line U-2932 was analyzed in depth. The cell line consists of two subclones with genomic and subgenomic aberrations including common (*BCL2*) and clone-specific (*MYC*) alterations [36]. The differential expression of over 60 genes in the two subclones could be traced back to genomic copy number variations or consequences of the differential expression of the transcription factor *BCL6* [37]. The immunoglobulin hypermutation patterns of both subclones were identified in the DNA from the primary material of the patient, confirming that the two clones of the cell line truly represented subclones of the tumor [36].

Immunoglobulin hypermutations occur in the dark zone of the germinal center. In the current study, we studied pre-germinal center B cells. Therefore, a hypermutation analysis could not be applied to identify subclones. Instead, we performed numerical analyses and next generation sequencing analyses. We found disease-characteristic aberrations that were common to both sister cell lines as well as mutations in one of the sisters only. Aberrations that affected both sisters included losses of *CDKN2A*, *CDKN2B*, *ETV6*, *IKZF1* and *PAX5*, all of them recurrent deletions in pre-B ALL (Table 1) [19,28,29,31,32]. *BCR-ABL1*, *ETV6-RUNX1* and *MEF2D-BCL9* are fusions that also occur recurrently in pre-B ALL [19,26]. At least one of the five pairs of cell lines expressed the corresponding fusion transcripts (Table 1). *MEF2D* (ex 5)—*BCL9* (ex 9) in YCUB-4 and YCUB-4R was especially noteworthy. *BCL9* is the most frequent fusion partner of *MEF2D* in pre-B ALL [26]. To our knowledge, this is the first description of a cell line expressing a *MEF2D-BCL9* fusion transcript. What is also novel is the *PAX5* R38H mutation (COSM5986423) in cell lines PC-53 and PC-53A (Table 1). *PAX5* mutations including point mutations are recurrent in B-cell ALL [28], and a

cell line carrying such a mutation might help to elucidate the pathogenetic sequelae of the mutation for the cell.

All point mutations, deletions and fusion transcripts described so far always affected both sister cell lines. When one sister carried a mutation, the other did so as well. Apparently, these mutations, characteristic for the disease, already existed in the originating tumor cell when the earlier sister cell line was established. None of them allowed one to distinguish between early and late sister cell lines.

The situation was different when we looked at copy number aberrations in toto, i.e., not specifically at deletions known to contribute to the disease. Then, additionally, most deletions and amplifications occurred in both sisters (Supplementary Table S2). However, 4/5 pairs of cell lines showed aberrations in one of the sisters only (Supplementary Table S2). Interestingly, earlier sister cell lines also carried specific aberrations (Supplementary Table S2). The expression of the *NSMAF-NUCKS1* fusion transcript in PC-53 was specific for the earlier sister (Table 1). Abnormalities in the chromosomal regions of *NSMAF* and *NUCKS1* in PC-53, but not in PC-53A, confirmed that the differential expression of the fusion transcript was caused at the molecular level (Supplementary Figure S6). This observation, as well as the observation that sister cell lines exhibit unique copy number alterations not shared by the other sister, suggest that the sister cell lines represent tumor clones that independently developed from an ancestor already carrying the mutations that are common to both sisters (Supplementary Table S2; the common alterations are highlighted in green).

Without DNA from the primary tumor, we could not formally exclude that the sister cell specific aberrations had developed in vitro. However, the WES analysis of *KRAS* and *NRAS* mutations in AT-1 and AT-2 suggests that both serial sister cell lines consist of two clones from the primary tumor. Both mutations, *KRAS* A146T (Gca/Aca; COSM19404) and *NRAS* G12C (Ggt/Tgt; COSM561), were detected in each of the sister cell lines, albeit at different percentages and not with the 50% wt vs. 50% mu read proportion that would be expected if a cell clone carried a wild-type and mutant version of a gene (Table 1, Supplementary Figures S8 and S9). It is highly unlikely that two identical mutations have occurred independently in vitro in two cell lines from one patient. Therefore, our data favor the view that two clones, one with the *KRAS* A146T and the other with the *NRAS* G12C mutation, had already existed in the patient. AT-1 and AT-2, established at first and second relapse, comprise both subclones, albeit at different percentages (Table 2).

In sum, the results of the RNA-seq, WES and CGH analyses of five pairs of sequential pre-B ALL cell lines show aberrations characteristic for the disease. Because they are unreported in cell lines so far, the *MEF2D-BCL9* fusion in YCUB-4 and YCUB-4R and the *PAX5* R38H mutation in PC-53 and PC-53A are noteworthy. Mutations specifically occurring in one of the sisters suggest a derivation from individual clones of the primary tumor, whereas common mutations point to the common ancestor. The study shows that sequential sister cell lines allow one to study common and clone-specific mutations.

**Supplementary Materials:** The following are available online at <https://www.mdpi.com/article/10.3390/cimb43030149/s1>, Figure S1: Fusion transcripts joining *ETV6* and *RUNX1*, Figure S2: Principal component analysis plot, Figure S3: *IKZF1* deletions, Figure S4: *CDKN2A/CDKN2B* deletions, Figure S5: *NSMAF/NUCKS1* fusion mRNA, Figure S6: Chromosomal aberrations affecting *NSMAF* and *NUCKS1*, Figure S7: *KRAS* and *NRAS* diploid in AT-1 and AT-2, Figure S8: *KRAS* A146T (Gca/Aca) mutation in AT-1 and AT-2, Figure S9: *NRAS* G12C (Gct/Tgt) mutation in AT-1 and AT-2, Table S1: Mutations and genomic aberrations of chromosome 14 in pre-B ALL sister cell lines, Table S2: Numerical aberrations according to CGH analysis, Table S3: Sequences of PCR primers.

**Author Contributions:** H.Q. analyzed the data and wrote the manuscript; C.P. performed all bioinformatic analyses; H.G.D. designed the study. All authors have read and agreed to the published version of the manuscript.

**Funding:** This research did not receive external funding.

**Data Availability Statement:** RNAseq (E-MTAB-11038) and WES data (E-MTAB-11039) were data were deposited at ArrayExpress.

**Acknowledgments:** The authors acknowledge the superb efforts of Vivien Hauer and Margarete Zaborski, technical assistants in the department.

**Conflicts of Interest:** The authors declare no conflict of interest.

## References

1. Ferreira, D.; Adega, F.; Chaves, R. The importance of cancer cell lines as in vitro models in cancer methylome analysis and anticancer drugs testing. In *Oncogenomics and Cancer Proteomics*; Lopez-Camarillo, C., Arechaga-Ocampo, E., Eds.; IntechOpen: London, UK, 2013.
2. Mirabelli, P.; Coppola, L.; Salvatore, M. Cancer cell lines are useful model systems for medical research. *Cancers* **2019**, *11*, 1098. [[CrossRef](#)]
3. Drexler, H.G.; Quentmeier, H. The LL-100 cell lines panel: Tool for molecular leukemia-lymphoma research. *Int. J. Mol. Sci.* **2020**, *21*, 5800. [[CrossRef](#)]
4. Waanders, E.; Gu, Z.; Dobson, S.M.; Antic, Z.; Chase Crawford, J.; Ma, X.; Edmonson, M.N.; Payne-Turner, D.; Van de Vorst, M.; Jongmans, M.C.J.; et al. Mutational landscape and patterns of clonal evolution in relapsed pediatric acute lymphoblastic leukemia. *Blood Cancer Discov.* **2020**, *1*, 96–111. [[CrossRef](#)] [[PubMed](#)]
5. Greaves, M. Evolutionary determinants of cancer. *Cancer Discov.* **2015**, *5*, 806–820. [[CrossRef](#)] [[PubMed](#)]
6. Ferrando, A.A.; Lopez-Otin, C. Clonal evolution in leukemia. *Nat. Med.* **2017**, *23*, 1135–1145. [[CrossRef](#)]
7. Lyne, A.M.; Laplane, L.; Perié, L. To portray clonal evolution in blood cancer, count your stem cells. *Blood* **2021**, *37*, 1862–1870. [[CrossRef](#)]
8. Drexler, H.G. *Guide to Leukemia-Lymphoma Cell Lines*, 2nd ed.; e-Book on CD; Drexler, H.G.: Braunschweig, Germany, 2010.
9. Dobin, A.; Davies, C.A.; Schlesinger, F.; Drenkow, J.; Zaleski, C.; Jha, S.; Batut, P.; Chaisson, M.; Gingeras, T.R. STAR: Ultrafast universal RNA-seq aligner. *Bioinformatics* **2013**, *29*, 15–21. [[CrossRef](#)]
10. Li, H.; Handsaker, B.; Wysoker, A.; Fennell, T.; Ruan, J.; Homer, N.; Marth, G.; Abecasis, G.; Durbin, R. 1000 Genome Project Data Processing Subgroup. The sequence alignment/map format and SAMtools. *Bioinformatics* **2009**, *25*, 2078–2079. [[CrossRef](#)] [[PubMed](#)]
11. Anders, S.; Pyl, P.T.; Huber, W. HTSeq—A Python framework to work with high-throughput sequencing data. *Bioinformatics* **2015**, *31*, 166–169. [[CrossRef](#)]
12. Anders, S.; Huber, W. Differential expression analysis for sequence count data. *Genome Biol.* **2010**, *11*, R106. [[CrossRef](#)] [[PubMed](#)]
13. Nicorici, D.; Satalan, M.; Edgren, H.; Kangaspeska, S.; Murumagi, A.; Kallioniemi, O.; Virtanen, S.; Kilkku, O. FusionCatcher—a tool for finding somatic fusion genes in paired-end RNA-sequencing data. *bioRxiv* **2014**, 011650. [[CrossRef](#)]
14. Pommerenke, C.; Geffers, R.; Bunk, B.; Bhujji, S.; Eberth, S.; Drexler, H.G.; Quentmeier, H. Enhanced whole exome sequencing by higher DNA insert lengths. *BMC Genom.* **2016**, *17*, 399. [[CrossRef](#)]
15. McKenna, A.; Hanna, M.; Banks, E.; Sivachenko, A.; Cibulskis, K.; Kernytzky, A.; Garimella, K.; Altshuler, D.; Gabriel, S.; Daly, M.; et al. The genome analysis toolkit: A MapReduce framework for analyzing next-generation DNA sequencing data. *Genome Res.* **2010**, *20*, 1297–1303. [[CrossRef](#)]
16. Koboldt, D.C.; Zhang, Q.; Larson, D.E.; Shen, D.; McLellan, M.D.; Lin, L.; Miller, C.A.; Mardis, E.R.; Ding, L.; Wilson, R.K. VarScan 2: Somatic mutation and copy number alteration discovery in cancer by exome sequencing. *Genome Res.* **2012**, *22*, 568–576. [[CrossRef](#)]
17. McLaren, W.; Pritchard, B.; Chen, Y.; Flicek, P.; Cunningham, F. Deriving the consequences of genomic variants with the Ensembl API and SNP effect predictor. *Bioinformatics* **2010**, *26*, 2069–2070. [[CrossRef](#)]
18. Shurtleff, S.A.; Buijs, A.; Behm, F.G.; Rubnitz, J.E.; Raimondi, S.C.; Hancock, M.; Chan, G.C.; Pui, C.H.; Grosveld, G.; Downing, J.R. TEL/AML1 fusion resulting from a cryptic t(12;21) is the most common genetic lesion in pediatric ALL and defines a subgroup of patients with an excellent prognosis. *Leukemia* **1995**, *9*, 1985–1989. [[PubMed](#)]
19. Mullighan, C.G. Molecular genetics of B-precursor acute lymphoblastic leukemia. *J. Clin. Invest* **2012**, *122*, 3407–3415. [[CrossRef](#)] [[PubMed](#)]
20. Uphoff, C.C.; MacLeod, R.A.F.; Denkmann, S.A.; Golub, T.R.; Borkhardt, A.; Janssen, J.W.G.; Drexler, H.G. Occurrence of TEL-AML1 fusion resulting from (12;21) translocation in human early B-lineage leukemia cell lines. *Leukemia* **1997**, *11*, 441–447. [[CrossRef](#)]
21. Fears, S.; Chakrabarti, S.R.; Nucifora, G.; Rowley, J.D. Differential expression of TCL1 during pre-B-cell acute lymphoblastic leukemia progression. *Cancer Genet. Cytogenet.* **2002**, *135*, 110–119. [[CrossRef](#)]
22. Kuiper, R.P.; Schoenmakers, E.F.P.M.; van Reijmersdal, S.V.; Hehir-Kwa, J.Y.; Geurts van Kessel, A.; van Leeuwen, F.N.; Hoogerbrugge, P.M. High-resolution genomic profiling of childhood ALL reveals novel recurrent genetic lesions affecting pathways involved in lymphocyte differentiation and cell cycle progression. *Leukemia* **2007**, *21*, 1258–1266. [[CrossRef](#)]
23. Matsuo, Y.; Ariyasu, T.; Ohmoto, E.; Kimura, I.; Minowada, J. Bi-phenotypic t(9;22)-positive leukemia cell lines from a patient with acute leukemia: NALM-20, established at the onset; and NALM-21, NALM-22 and NALM-23, established after relapse. *Hum. Cell* **1991**, *4*, 335–338. [[PubMed](#)]

24. Uphoff, C.C.; Habig, S.; Fombonne, S.; Matsuo, Y.; Drexler, H.G. ABL-BCR expression in BCR-ABL-positive human leukemia cell lines. *Leuk. Res.* **1999**, *23*, 1055–1060. [[CrossRef](#)]
25. Ariyasu, T.; Matsuo, Y.; Harashima, A.; Nakamura, S.; Takaba, S.; Tsubota, T.; Orita, K. Establishment and characterization of “biphenotypic” acute leukemia cell lines with a variant Ph translocation t(9;22;10) (q34;q11;q22). *Hum. Cell* **1998**, *11*, 43–50. [[PubMed](#)]
26. Gu, Z.; Churchman, M.; Roberts, K.; Li, Y.; Liu, Y.; Harvey, R.C.; McCastlain, K.; Reshmi, S.C.; Payne-Turner, D.; Iacobucci, I.; et al. Genomic analyses identify recurrent MEF2D fusions in acute lymphoblastic leukaemia. *Nat. Commun.* **2016**, *7*, 13331. [[CrossRef](#)]
27. Goto, H.; Naruto, T.; Tanoshima, R.; Kato, H.; Yokosuka, T.; Yanagimachi, M.; Fujii, H.; Yokota, S.; Komine, H. Chemo-sensitivity in a panel of B-cell precursor acute lymphoblastic leukemia cell lines, YCUB series, derived from children. *Leuk. Res.* **2009**, *33*, 1386–1391. [[CrossRef](#)] [[PubMed](#)]
28. Mullighan, C.G.; Goorha, S.; Radtke, I.; Miller, C.B.; Coustan-Smith, E.; Dalton, J.D.; Girtman, K.; Mathew, S.; Ma, J.; Pounds, S.B.; et al. Genome-wide analysis of genetic alterations in acute lymphoblastic leukaemia. *Nature* **2007**, *446*, 758–764. [[CrossRef](#)] [[PubMed](#)]
29. Zhang, X.; Rastogi, P.; Shah, B.; Zhang, L. B lymphoblastic leukemia/lymphoma: New insights into genetics, molecular aberrations, subclassification and targeted therapy. *Oncotarget* **2017**, *8*, 66728–66741. [[CrossRef](#)]
30. Tarella, C.; Pregno, P.; Gallo, E.; Caracciolo, D.; Stefani, S.; Barletta, C.; Lanfrancone, L.; Ferrero, D. Establishment from an adult leukemic patient of two novel precursor B cell lines with different growth modality. *Leuk. Res.* **1990**, *14*, 177–184. [[CrossRef](#)]
31. Iacobucci, I.; Iraci, N.; Messina, M.; Lonetti, A.; Chiaretti, S.; Valli, E.; Ferrari, A.; Papayannidis, C.; Paolini, F.; Vitale, A.; et al. IKAROS deletions dictate a unique gene expression signature in patients with adult B-cell acute lymphoblastic leukemia. *PLoS ONE* **2012**, *7*, e40934. [[CrossRef](#)] [[PubMed](#)]
32. Ribera, J.; Zamora, L.; Morgades, M.; Vives, S.; Granada, I.; Montesinos, P.; Gómez-Seguí, I.; Mercadal, S.; Guàrdia, R.; Nomdedeu, J.; et al. Molecular profiling refines minimal residual disease-based prognostic assessment in adults with Philadelphia chromosome-negative B-cell precursor acute lymphoblastic leukemia. *Genes Chromosomes Cancer* **2019**, *58*, 815–819. [[CrossRef](#)] [[PubMed](#)]
33. Stanulla, M.; Cavé, H.; Moorman, A.V. IKZF1 deletions in pediatric acute lymphoblastic leukemia: Still a poor prognostic marker? *Blood* **2020**, *135*, 252–260. [[CrossRef](#)]
34. Hof, J.; Krentz, S.; van Schewick, C.; Körner, G.; Shalapour, S.; Rhein, P.; Karawajew, L.; Ludwig, W.D.; Seeger, K.; Henze, G.; et al. Mutations and deletions of the TP53 gene predict nonresponse to treatment and poor outcome in first relapse of childhood acute lymphoblastic leukemia. *J. Clin. Oncol.* **2011**, *29*, 3185–3193. [[CrossRef](#)] [[PubMed](#)]
35. Quentmeier, H.; Pommerenke, C.; Ammerpohl, O.; Geffers, R.; Hauer, V.; MacLeod, R.A.F.; Nagel, S.; Romani, J.; Rosati, E.; Rosén, A.; et al. Subclones in B-lymphoma cell lines: Isogenic models for the study of gene regulation. *Oncotarget* **2016**, *7*, 63456–63465. [[CrossRef](#)] [[PubMed](#)]
36. Quentmeier, H.; Amini, R.M.; Berglund, M.; Dirks, W.G.; Ehrentraut, S.; Geffers, R.; MacLeod, R.A.F.; Nagel, S.; Romani, J.; Scherr, M.; et al. U-2932: Two clones in one cell line, a tool for the study of clonal evolution. *Leukemia* **2013**, *27*, 1155–1164. [[CrossRef](#)] [[PubMed](#)]
37. Ding, J.; Dirks, W.G.; Ehrentraut, S.; Geffers, R.; MacLeod, R.A.F.; Nagel, S.; Pommerenke, C.; Romani, J.; Scherr, M.; Vaas, L.A.I.; et al. BCL6-regulated by AhR/ARNT and wild-type MEF2B-drives expression of germinal center markers MYBL1 and LMO2. *Haematologica* **2015**, *100*, 801–809. [[CrossRef](#)]